Cretaceous Research 145 (2023) 105472

Contents lists available at ScienceDirect

Cretaceous Research

journal homepage: www.elsevier.com/locate/CretRes

Lower Cretaceous Hailar amber: The oldest-known amber from China

Yuling Li [a, b], Daran Zheng [a], Jingeng Sha [a], Haichun Zhang [a], Steven Denyszyn [c], Su-Chin Chang [b, *]

[a] State Key Laboratory of Palaeobiology and Stratigraphy, Nanjing Institute of Geology and Palaeontology, Chinese Academy of Sciences, 39 East Beijing Road, Nanjing 210008, China
[b] The Department of Earth Sciences, The University of Hong Kong, Hong Kong, China
[c] Department of Earth Sciences, Memorial University of Newfoundland, Canada

ARTICLE INFO

Article history:
Received 28 September 2022
Received in revised form
16 December 2022
Accepted in revised form 30 December 2022
Available online 2 January 2023

Keywords:
In-situ amber
Zhalainuoer coal mine
Yimin Formation
Hailar Basin
U–Pb geochronology

ABSTRACT

Amber deposits provide a rare opportunity to look into the details of terrestrial ecosystems. This study reviews six well-documented Chinese amber deposits from the Mesozoic to Cenozoic, and reviews Cretaceous amber deposits globally. The discovery of *in situ* ambers from the Yimin and Zhalainuoer coal fields in the Hailar Basin extends the geographic distribution of Chinese amber outcrops into northeast China. Stratigraphic correlation and U–Pb geochronology indicate that the Hailar ambers formed in the Early Cretaceous and thus represent the oldest-known amber in China, a unique window into the paleoenvironments of the Cretaceous world. Further investigations into the amber-bearing Yimin Formation will advance understanding of Cretaceous biotas, local ecosystems, global environmental change, and the link between biology and climate.

1. Introduction

Amber is a fossilized tree resin ranging from a few million to 320 million years (Bray and Anderson, 2009). Amber is found worldwide, from the Arctic to Antarctica. As far back as the Neolithic period, around 13,000 years ago, humans have valued amber for its color and natural beauty (Grimaldi, 2009, 2019). Amber has a long history of utilization as ornaments across cultures and has been interpreted to have healing powers in many regions. In China, amber is called Hu-Po, which means "spirit of the tiger." According to archaeological data, the earliest known human use of amber in China occurs in the first sacrificial pit discovered at the Sanxingdui site, which was active during the Shang Dynasty ~3000 years ago (Chen et al., 2019). The earliest written record of amber in China dates from the Han Dynasty, around 200 BC, indicating that amber was as precious as gold and jade (Huo and Zhao, 2007). Amber artifacts dating back to that period have been discovered in many localities in China, especially in southern China (Chen et al., 2019). In addition to its use as a gemstone, amber has been used in traditional Chinese medicine over the past ~1500 years. Lei's Treatise on the Preparation of Medicinal Substances (Lei Gong Pao Zhi Lun, ~5th century) describes the medical benefits of amber as supporting mental stability, hemostasis, healing of wounds, and diuresis. Due to the high demand for amber, historical records document the import of amber mainly from Myanmar and the Baltic region since the Han Dynasty (Laufer, 1906; Qin and Sun, 2016; Chen et al., 2019). Although the history and scale of amber mining activities in ancient China remain unclear, localities producing amber have been well-known since at least the 19th century (Qin and Sun, 2016). The study of inclusions in Chinese amber began in the 1970s, and research on the Eocene Fushun amber deposits in northeast China started in the 1980s (Hong et al., 1974; Hong, 2002). After the 6th International Congress on Fossil Insects, Arthropods and Amber held in Lebanon (2013), scientific interest in amber and its inclusions expanded significantly among Chinese and other research communities (Azar et al., 2019). Consequently, Chinese institutions, particularly the Nanjing Institute of Geology and Palaeontology, the Chinese Academy of Sciences, acquired extensive collections from Chinese and other international sources. Recently, Wang et al. (2021a) described the Zhangpu amber from a Miocene outcrop in Fujian, southeast China, with abundant fossil inclusions.

This paper reviews Chinese amber sites reported in peer-reviewed scientific publications. We also report on two newly

* Corresponding author.
E-mail address: suchin@hku.hk (S.-C. Chang).

https://doi.org/10.1016/j.cretres.2022.105472
0195-6671/

discovered amber sites from the Lower Cretaceous Zhalainuoer Group in the Hailar Basin of Inner Mongolia, northeast China. We characterized the Hailar amber using micro-Fourier-transform infrared spectroscopy (FTIR). New U–Pb ages for detrital zircons from the amber-bearing beds, along with previous biostratigraphic correlations within the Hailar Basin, indicate that the amber is ~130 Ma or the latest Hauterivian in age. This study of both local and regional amber expands our understanding of Early Cretaceous paleo-ecosystems and paleoenvironment in North China. It demonstrates research directions and can guide future research on Chinese amber.

2. Amber sites in China

Although the Chinese have a long history of trading and using amber, few systematic investigations of amber sites have been conducted in China. Until now, only a few amber localities have been described or reported, including Zhangpu in Fujian, Lunpola in northern Tibet, Nanning in Guangxi, Fushun in Liaoning, Xixia in Henan, and Manzhouli (Manchuria) in Inner Mongolia. Wang et al. (2011) mentioned several amber sites, such as Daohugou, Jiayin, Yanbian, and Ganglong. However, none of these sites have been formally studied and documented. For the first time, this paper reviews amber sites that have been described in scientific journals, and it reports on two newly discovered amber sites from Hailar Basin in Inner Mongolia Autonomous Region (Fig. 1).

Zhangpu amber: This amber occurs within the Miocene Fotan Group in Fujian Province, southeast China. Until the 21st century, Zhangpu amber garnered little attention due to its fragility and physical properties which were unsuitable for making jewelry (Shi et al., 2014a). Wang et al. (2021a) recently described a middle Miocene rainforest biome, and a biota named the Zhangpu biota based on material preserved in the Zhangpu amber. From approximately 25,000 fossil-containing amber samples and 5000 co-occurring plant fossils, the Zhangpu biota represents the richest tropical seasonal rainforest biota discovered thus far in the fossil record. A wide range of inclusions from the ambers provided biodiversity estimates and demonstrated the northerly expansion of tropical rainforests in East Asia (Zheng et al., 2019a; Li et al., 2021; Wang et al., 2021c; Brazidec and Perrichot, 2022; Chen et al., 2022). Amber inclusions hosted plants, gastropods, and vertebrates with exquisite preservation. These provide a window into ecosystem dynamics during the Mid-Miocene Climatic Optimum (MMCO, ~14–17 Ma) (Wang et al., 2021a, 2021c). A range of critical and high-profile fossil inclusions from the Zhangpu amber has drawn considerable scientific and media attention. For example, at least 200 families of insects belonging to 20 orders have been

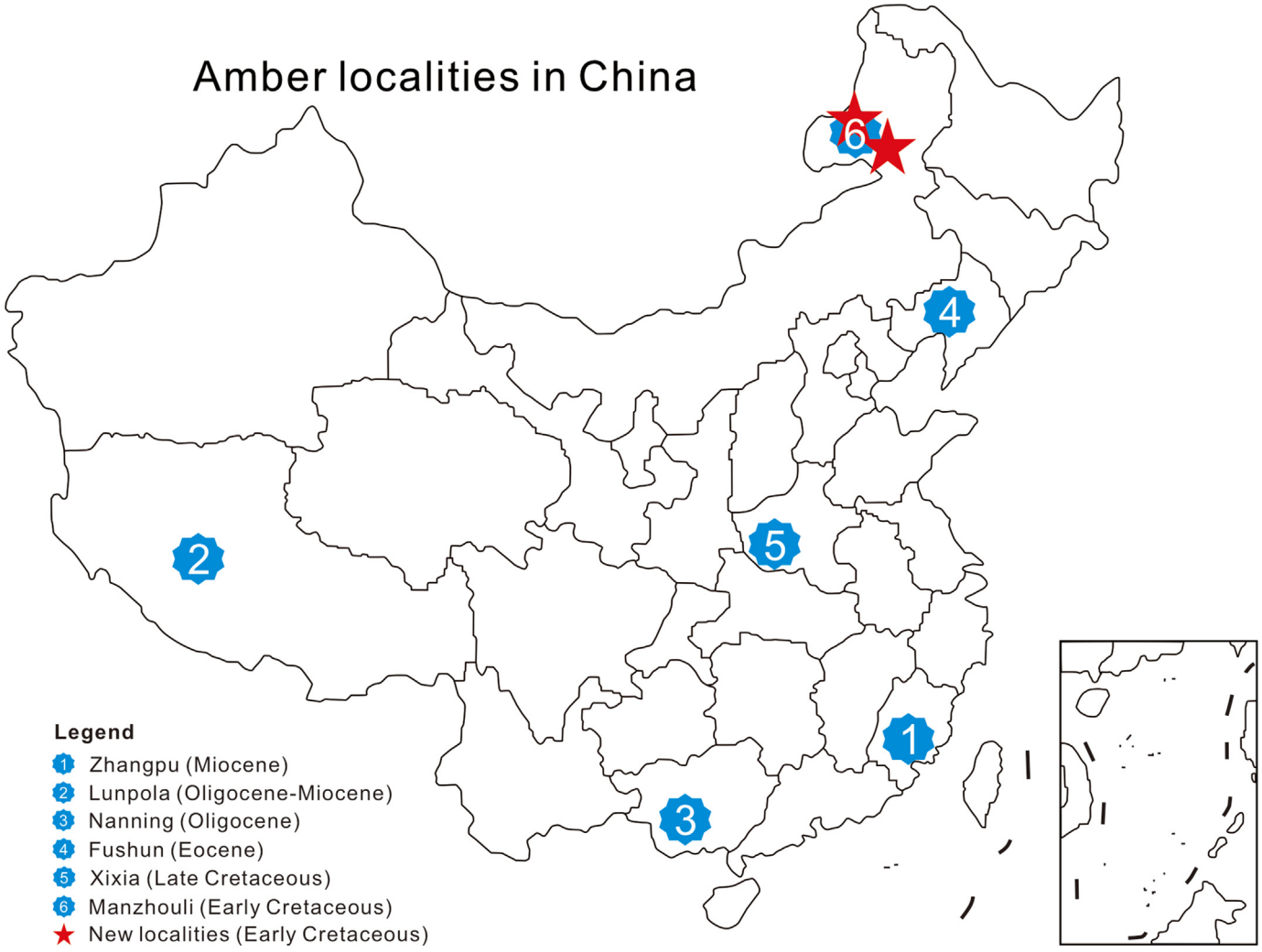

Fig. 1. Map showing the geographic distribution of Chinese amber (only formally reported localities).

identified, making the Zhangpu amber biota one of the world's four richest amber biotas (Engel et al., 2021; Wang et al., 2021a).

Lunpola amber: The amber layer was discovered in the upper Oligocene to lower Miocene Dingqing Formation of the Lunpola Basin, central Tibet in 2018 (Wang et al., 2018). The amber pieces are usually less than 1 cm in diameter, and embedded in grey mudstone. Analyses of biomarkers indicate that the Lunpola amber originated from dipterocarps, which now represent the most dominant trees in Asian tropical rainforests. Although inclusions have not been reported from this amber, the resin's biomarkers suggest that the tropical rainforest existed in the northern part of the Lhasa Terrane (central Tibet) at an elevation of less than 1300 m above sea level around 40 million years ago (Wang et al., 2018). The Lunpola amber thus contains clues concerning the uplift history of the Tibetan Plateau, which exerted a significant influence on East Asian climate and biodiversity (Wu et al., 2015). The finding of dipterocarp-derived amber provides further support for the hypothesis of India as the origin of Asian dipterocarps in the Early Cenozoic (Dutta et al., 2011; Shi et al., 2014a,b).

Nanning amber: An Oligocene amber outcrop from the Nanning Basin of Guangxi was reported in a preliminary study (Liu et al., 2021). Fifty-seven small amber pieces were collected from an open pit outcrop of the fossil-rich upper Yongning Formation. A vibrant fauna with diverse gastropods, bivalves, fish fragments, and crocodile teeth occurs nearby (Tian et al., 2018). The amber appears dark brown in color but nearly transparent under intense light. No inclusions have been found in the Nanning amber. This amber also lacks detailed geological study and robust age determination.

Fushun amber: The early Eocene Fushun amber of Liaoning Province occurs in what was one of the largest opencast coal mines in Asia. This deposit has been known for over a century and was traditionally regarded as an essential source of medicinal and organic gemstones. Despite the Fushun amber's commercial value, its inclusions have not been comprehensively investigated. Although Ping (1931) and Hong (2002) described some insect inclusions from the Fushun amber, its paleobiota and scientific significance remained understudied until the early 21st century (Rust et al., 2010). Wang et al. (2014) provided the first detailed overview of Fushun amber biota before the coal mine closed after 110 years of operation. A study on amber's chemistry revealed conifers of the cypress family (Cupressaceae) as its likely origin since the remains of these trees commonly occur as fossils in the Fushun amber-bearing beds and as inclusions in the amber. In addition to insect remains, plants, fungi, amoebae, and mammal hairs have also been found in the amber (Ross, 2014; Wang et al., 2014). The most important results from the Fushun amber biota have been the constraints provided on the biogeographic ranges of several biotas. The detailed profile of inclusions also indicates biotic exchange between the eastern and western margins of the Eurasian landmass during the Eocene (Wang et al., 2014; Zhang et al., 2016; Stebner et al., 2017; Azar et al., 2018).

Xixia amber: The Xixia amber, from the Late Cretaceous Gaogou Formation in Henan Province, Central China, was known and mined before 1949 (Zhou and Zhao, 2005). Due to its poorly consolidated texture, the Xixia amber does not qualify as a gemstone and is mainly used for medicine. Molecular compositional analysis indicates that the Xixia amber derives from the conifer family Araucariaceae, a type of plant that widely occurred in the Northern Hemisphere during the Mesozoic (Shi et al., 2014a). Although fossil inclusions have not been reported from the Xixia amber, they may exist since abundant, well-preserved dinosaurs, turtles, dinosaur eggs, and turtle eggs have been discovered from the same formation (Wang et al., 2006; Chen et al., 2007; Zheng et al., 2015; Pu et al., 2017; Xu et al., 2022).

Lingquan amber: In 2019, a piece of amber was described from the Lingquan coal mine in Manzhouli in northeast China's Inner Mongolia (Azar et al., 2019). This millimeter-scale amber was found in the Lower Cretaceous Damoguaihe Formation. Although a preliminary study was not able to identify the botanical origin of this amber, Azar et al. (2019) noted that any amber discovered from Early Cretaceous deposits could fill critical chronostratigraphic and biostratigraphic gaps among several higher profile amber deposits, for example the Lebanese amber (Barremian) (Azar, 2007, 2012) as well as late Albian to Cenomanian ambers from Spain, France, and Myanmar (Alonso et al., 2000; Arillo and Subías, 2000, 2002; Zheng et al., 2018).

During our field excavation in the summer of 2019, we discovered two new amber sites: one found at the Zhalainuoer coal mine and the other at the Yimin coal mine. Since both sites are located in the Hailar Basin of Inner Mongolia in the northern portion of northeast China (Fig. 2A), we refer to them collectively as Hailar amber. This study describes sampling localities in detail and discusses the local and global implications for the Early Cretaceous amber.

3. Geological setting and sampling

Extensional structures characterize the geological landscape of northeast China during the Jurassic and Cretaceous (Graham et al., 2001; Dong et al., 2015; Ouyang et al., 2015). A series of important petroliferous, fault-bounded basins, including the Hailar-Tamtsag, Songliao, and Erlian basins, also formed during this period (Meng et al., 2003; Hou et al., 2008; Cao et al., 2009; Sun et al., 2018; Ji et al., 2019; Song et al., 2019; Suo et al., 2020).

The ~40,550 km^2 Hailar Basin occurs within the Central Asian Orogenic Belt, which is located between the Siberian craton to the north and the North China-Mongolian craton to the south (Ji et al., 2019). This intra-cratonic basin exhibits NE-SW oriented faults predominantly. It contains up to 4–5 km of Late Mesozoic to Cenozoic nonmarine sediments and 16 sags that formed synchronously within an extensional tectonic regime (A et al., 2013). The fault-bound Hailar basin extends into Mongolia as the Tamstag Basin (Zhang and Long, 1995; Meng et al., 2003; Jia et al., 2019). Since the early 21st century, the sedimentary evolution and thermal history of the Hailar Basin have been a focus of study due to the basin's energy resource potential (Huang et al., 2006; Wu et al., 2006; Cao et al., 2009; A et al., 2013; Xia et al., 2017; Li et al., 2018; Ji et al., 2020, 2021; Wang et al., 2021b).

The Hailar Basin can be divided into several tectonic units (Fig. 2B). Thick sediments were deposited from the Jurassic to Early Cenozoic (Fig. 2C). Despite intensive natural resource exploration, much work remains to be done. For example, systematic correlations and a stratigraphic framework for the basin are lacking. Different lithostratigraphic subdivisions have been described for the Jurassic-Cretaceous units in the Hailar Basin (Zhang and Long, 1995; A et al., 2013; Guo et al., 2018; Ji et al., 2019; Song et al., 2019; Zhu et al., 2019). This study used A et al.'s (2013) framework since it represents a compilation of previous stratigraphic frameworks that include clear sedimentological records for the area.

The Cretaceous Zhalainuoer Group is divided into the Damoguaihe and Yimin formations (Fig. 2C). In ascending order, the Damoguaihe Formation consists of clastic sedimentary deposits with a layers of coal or clastic horizons composed of conglomerate, sandstone, siltstone, mudstone, and tuff. The Yimin Formation is a coal-bearing deposit that overlies the Damoguaihe Formation (IMARBGMR, 1996; Azar et al., 2019). The Yimin Formation accumulated in a depocenter experiencing milder tectonic activity.

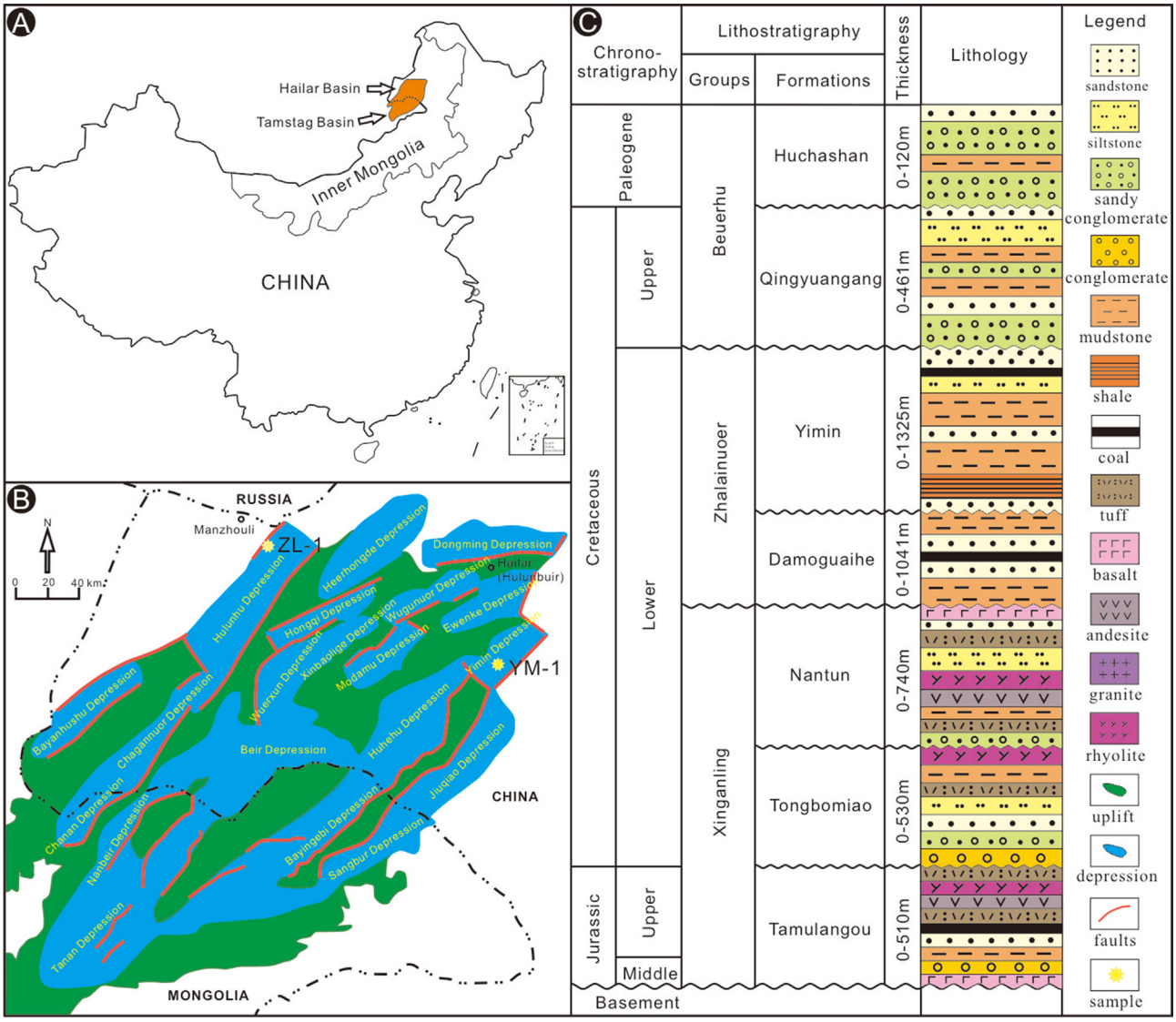

Fig. 2. (A) Geographic sketch map of China showing the location of the Hailar Basin. (B) Tectonic units of the Hailar-Tamtsag Basin. The Hailar Basin extends into Mongolia is called the Tamtsag Basin (modified after Ji et al., 2019). (C) Stratigraphic column for the Hailar Basin (modified after A et al., 2013 and Ji et al., 2019).

Thick coal seams are widely distributed throughout the formation as part of lacustrine transgression and high-stand systems tracts (Guo et al., 2014; Zhang et al., 2015). Based on fossil records, most previous studies interpret an Early Cretaceous age for both formations. However, different interpretations exist and radioisotopic age constraints for both coal-bearing formations are rare and imprecise (Pu and Wu, 1985; Wan, 2006; Zhou et al., 2014; Ji et al., 2019). For example, a government report (IIMARBGMR, 1996) suggested that animal fossils from the Damoguaihe Formation represent a late stage of the Jehol Biota (i.e. Barremian to early Aptian). Meanwhile, Pu and Wu (1985) and Cheng and Shang (2015) interpreted the Damoguaihe Formation as Valanginian–Barremian in age based on its palynological assemblages. Wang et al. (2012) provided an Aptian age according to ostracod assemblages. Previous paleontological studies interpret the Yimin Formation as probably deposited between Barremian and Albian epochs (Pu and Wu, 1985; Wan et al., 2005). Palynological records from the Yimin Formation show that its vegetation input is derived mainly from coniferous forests and shrubs such as hygrophilous Cyathidites and Pilosisporites, which indicate a humid tropical climate (Zhang and Long, 1995; Wang et al., 2008).

We collected hundreds of pieces of amber and tuffaceous sandstones from the Yimin Formation around the Zhalainuoer coal mine (N 49°27′8″, E 117°44′13″ E) and Yimin coal field (N 48°35′20″, E 119°44′20″ E) (Figs. 3, 4). The Zhalainuoer coal fields occupy an area of about 480 km^2 located in a northerly region of the Zhalainuoer Depression. The Yimin coal field represents the most important coal production site and power plant in the Hulunbeier City of Inner Mongolia. It is located in the middle and eastern part of the Yimin Fault Depression and occupies an area of approximately 600 km^2. Although both amber horizons occur within the Yimin Formation, about 200 km separates the sample localities, thus obscuring their exact stratigraphic relations.

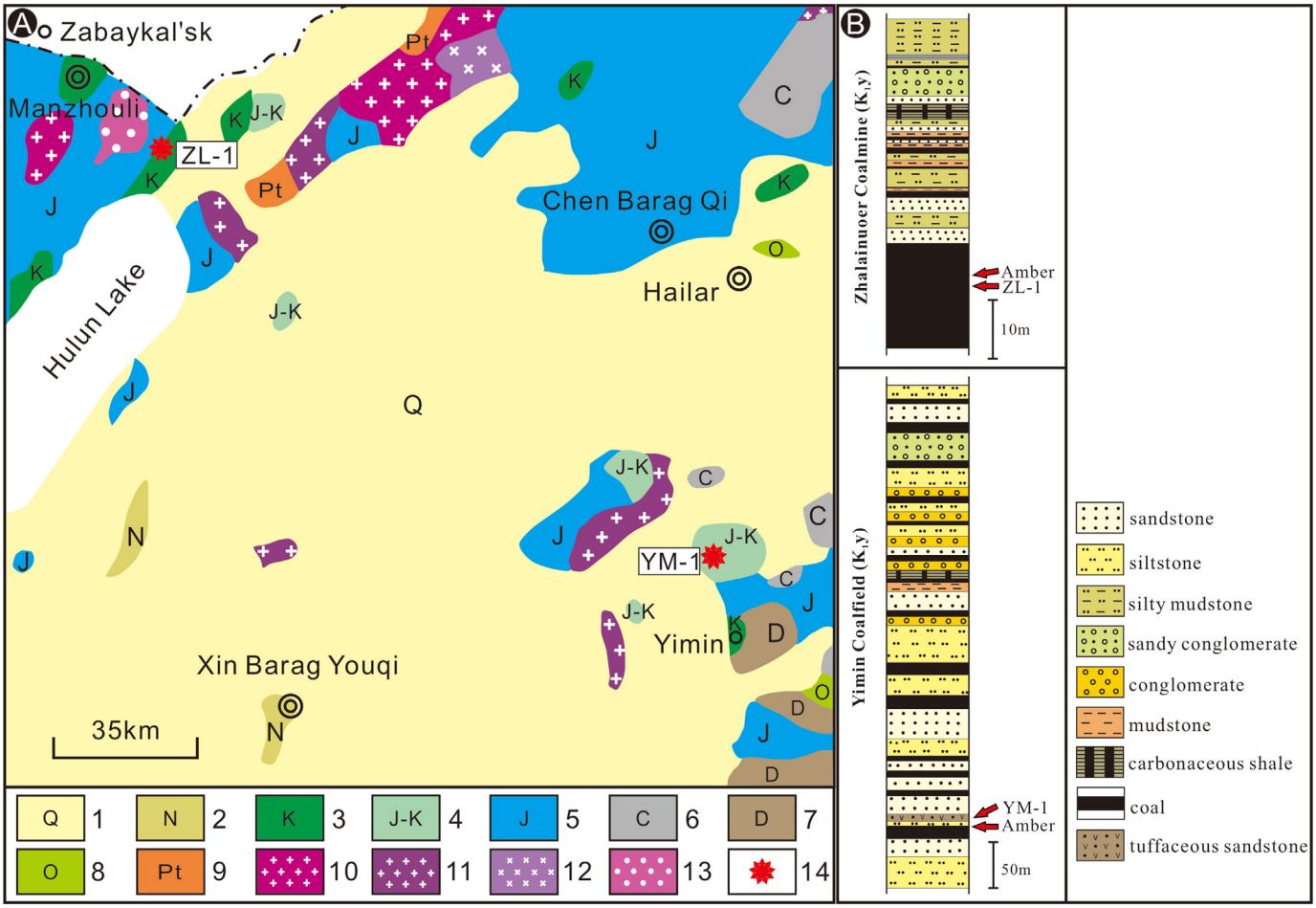

Fig. 3. (A) Geological map of the Hailar Basin and adjacent areas (after Geological Atlas of China, 2002). Key to symbols: 1) Quaternary; 2) Neogene; 3) Cretaceous; 4) Upper Jurassic ~ Lower Cretaceous; 5) Jurassic; 6) Carboniferous; 7) Devonian; 8) Ordovician; 9) Proterozoic; 10) Yanshanian granite; 11) Variscan granite; 12) Yanshanian granodiorite; 13) Yanshanian quartz monzonite; 14) Samples. (B) Stratigraphic columns show the Yimin Formation's lithology at the Zhalainuoer coal mine and Yimin coal field. Red arrows show the position of the amber and dated samples.

4. Amber analysis

More than 100 amber pieces were collected from the Cretaceous Yimin Formation at the Zhalainuoer coal mine and Yimin coal field. These specimens were deposited at the Nanjing Institute of Geology and Palaeontology, Chinese Academy of Sciences (NIGPAS).

The amber pieces from both outcrops described in this study are usually tiny, brown-colored and brittle, and thus do not qualify as gem quality. Specimens were photographed using a Zeiss Stereo Discovery V16 microscope system at NIGPAS (Fig. 5). Imaging consisted of digitally stacking photomicrographs into composites of approximately 40 individual focal planes using the image-editing software Helicon Focus 6 (www.heliconsoft.com).

To investigate the amber's botanical source, selected amber pieces were analyzed by Micro-Fourier-transform infrared (FTIR) using the Thermo Scientific™ Nicolet™ iN10 with K–Br pellets at Shiyanjia Lab, China (www.shiyanjia.com). The resin was cleared of all potential inclusions, contamination, and surface alterations, then crushed and transferred to a well mount. The absorbance spectrum was measured across a 4000–500 cm^{-1} wavelength range. The spectra were corrected with baseline ATR. Supplementary Table 1 lists raw FTIR data. Fig. 6 presents FTIR spectra for the two amber samples, ZL009 and ZL010. Absorption features and spectra for each sample resembled each other in displaying similar peaks of similar relative intensity. Hydroxyl (–OH) stretching of alcohols and acids appears as a broad, shallow peak at 3404 cm^{-1}. Adjacent alkyl stretching peaks appear at around 2931 and 2860 cm^{-1} corresponding to $-CH_2$ and $-CH_3$ stretching, respectively. Two additional alkyl peaks occur at 1443 and 1378 cm^{-1} and are attributed to $-CH_2$ and $-CH_3$ bending and $-CH_3$ bending, respectively. Prominent absorption peaks in both spectra occur at 1734 and 1703 cm^{-1} corresponding to carbonyl (–C=O) stretching from carboxylic acid groups. The region from 1300 to 1100 cm^{-1} was interpreted as stretching from single bonded –C–O groups in acids, alcohols, and esters. Spectral features below wavelengths of 1100 cm^{-1} could not be consistently interpreted.

The spectra for the Hailar amber appear unique from those of known ambers analyzed from other localities (Table 1). Although the wide fire occurred during the period when the Hailar amber was formed, we did not observe any alteration in the spectra. Results indicate that the Hailar amber pieces originated from coniferous plants but cannot be assigned to specific or extant conifer families.

5. Zircon U–Pb geochronology

Two tuffaceous sandstones (ZL-1 and YM-1) were collected from the upper part of the Yimin Formation at the Zhalainoer amber site and from the lowest part of the Yimin Formation at the Yimin amber site. For zircon extraction, samples were crushed and

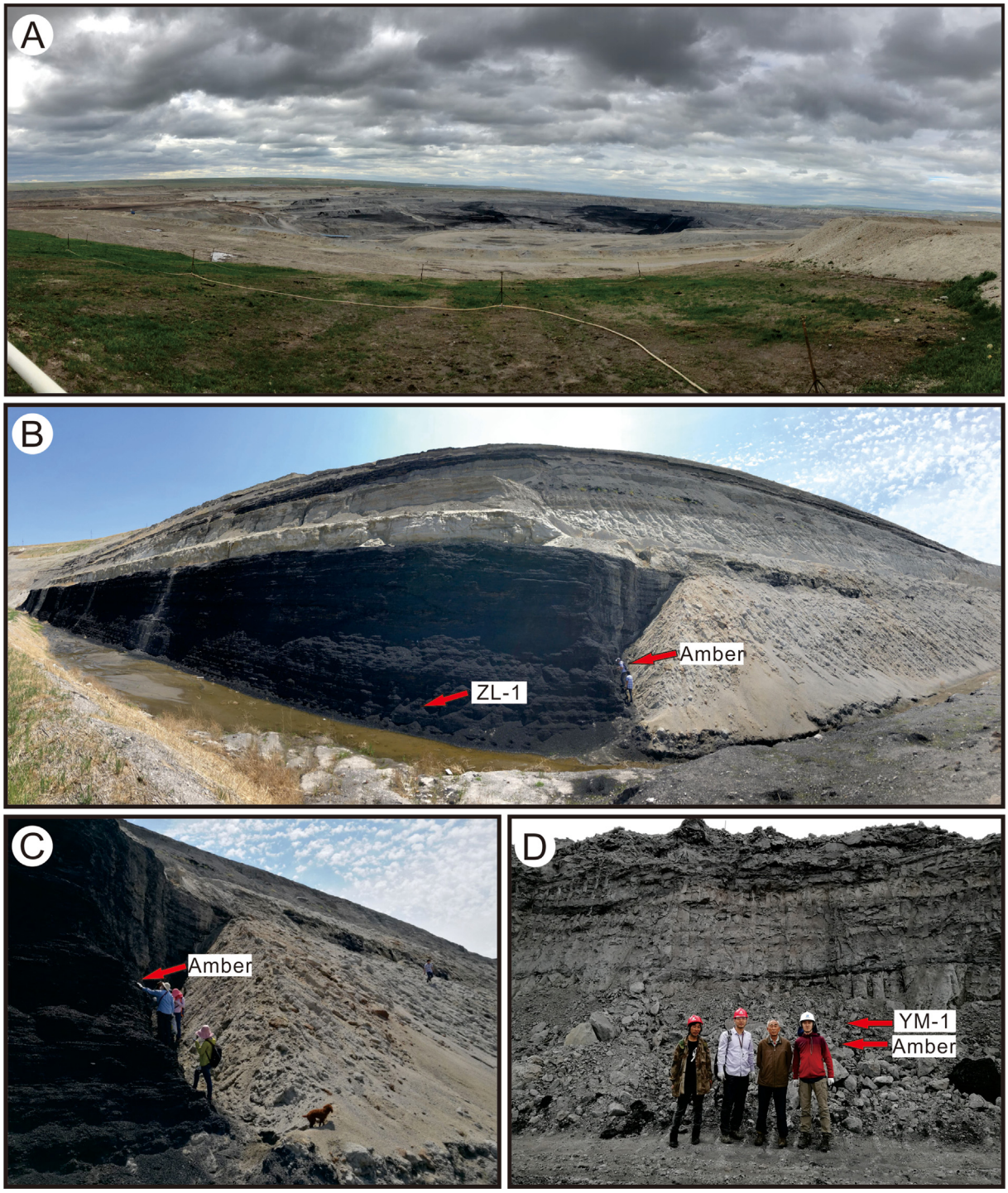

Fig. 4. Outcrop photos of Zhalainuoer coal mine (N 49° 27′ 8″, E 117° 44′ 13″) (B and C) and Yimin coal field (N 48° 35′ 20.09″, E 119° 44′ 20.39″) (A and D). Arrows indicate the sample site.

subjected to standard sieving and magnetic and heavy liquid separation techniques. A total of 100 inclusion-free zircon grains (80–200 μm) from samples were then hand-picked under a binocular microscope and mounted in epoxy resin. Hardened mounts were polished to expose zircon grain mid-sections at about 2/3 to 1/2 of their width. Cathodoluminescent (CL) imaging documented grain morphologies and internal structure for *in situ* analysis.

Zircons were analyzed for U–Pb isotopes using a LA-ICP-MS at the Metal Isotope Geochemistry Laboratory, University of Waterloo. The Agilent 8800 triple-quadrupole ICPMS and a Photon Machines Analyte G2 laser-ablation system used a 50 μm diameter beam generated at 7 Hz and 3 J/cm^2 as a source. A pre-ablation process was used to clear zircon surfaces over an area larger area than the analytical beam diameter. A 10 s baseline measurement was followed by 28 s of data collection and 20 s of washout. Measured

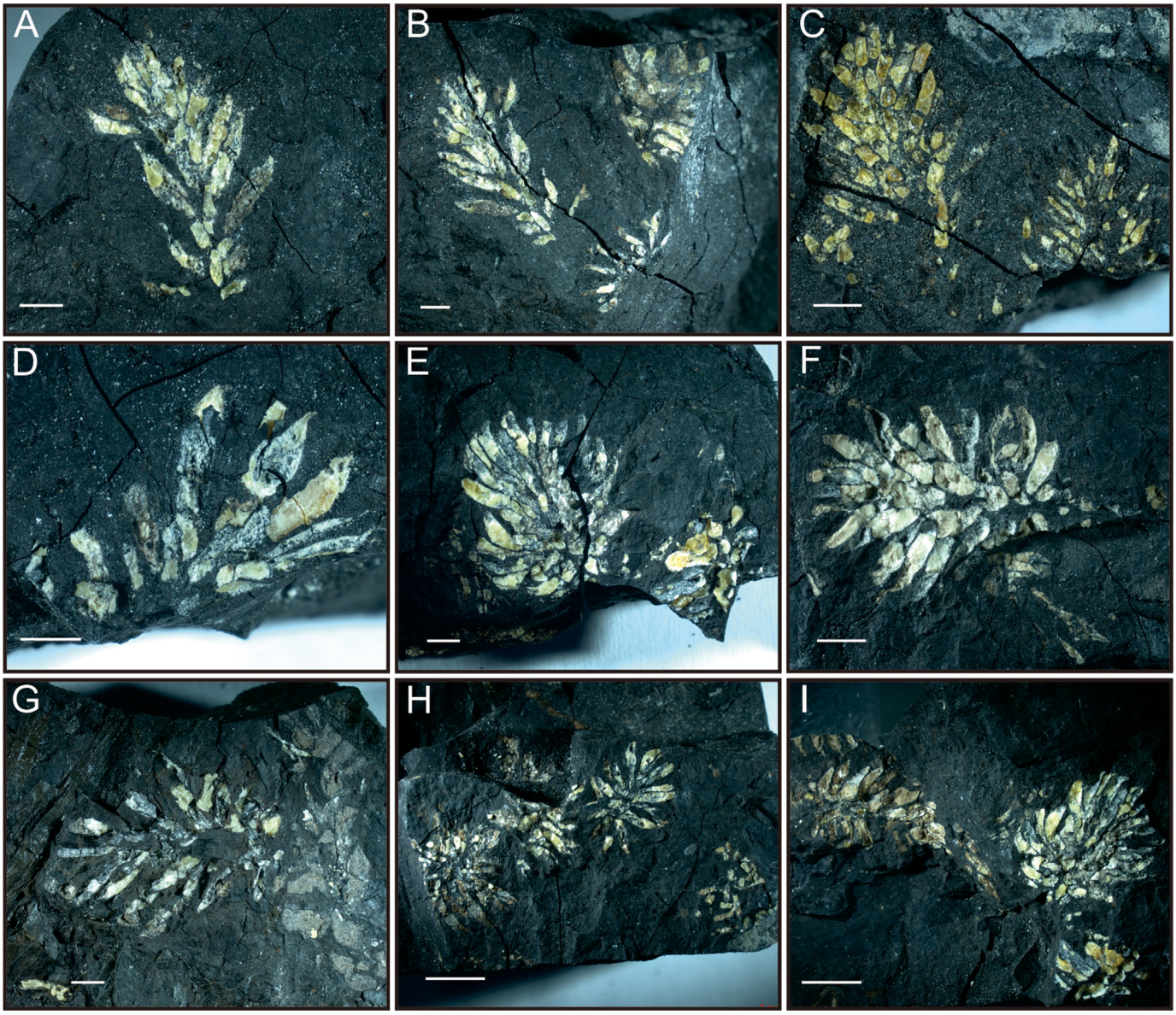

Fig. 5. Micrographs of amber from Zhalainuoer coal mine (A-F, H-I) and Yimin coal field (G). A-G, scale bars = 2 mm. H-I, scale bars = 5 mm.

masses of ^{88}Sr, ^{206}Pb, ^{207}Pb, ^{232}Th, and ^{238}U were reduced using the Iolite v. 3.6 software package. Data reduction included an exponential downhole fractionation correction. No common Pb correction was made due to negligible measured levels of ^{204}Pb. ^{88}Sr was measured to assess the presence of inclusions or alteration zones in zircons. Portions of the signal with high Sr or erratic beam behavior were avoided by restricting the selected time window or were otherwise rejected. Zircon 91500 (Wiedenbeck et al., 1995) served as a primary standard and zircons Plesovice (Sláma et al., 2008) and Temora (Black et al., 2003) served as secondary standards. Standard analyses bracketed every five to six sample measurements. Age calculations used U decay constants from Jaffey et al. (1971) and U isotopic composition from Steiger and Jäger (1977). Supplementary Table 2 shows U–Pb data with 2σ uncertainties.

We analyzed 52 and 43 zircon grains respectively from sandstone samples ZL-1 and YM-1, which occurred directly above the amber-bearing layers. With a few exceptions, zircon grains ranged from 80 to 160 μm in size. Most grains exhibited euhedral morphologies and oscillatory zoning patterns indicating igneous origin. Four grains from the youngest age population of ZL-1 provided a weighted mean value of 111.7 ± 2.2 Ma (MSWD = 6.9; 2σ) and four grains from the youngest age population of YM-1 provided a weighted mean value of 130.9 ± 2.8 Ma (MSWD = 3.3; 2σ) (Fig. 7). The latter age was interpreted as the maximum depositional age for the lowest part of the Yimin Formation.

6. Discussion

6.1. Origin of the Hailar amber

Amber is a fossilized natural resin produced by ancient plant secretory cells. In addition to its human ornamental and medicinal uses, it also can provide unique preservation of small-scale fossil material and soft-bodied microorganisms (Schmidt et al., 2006; Rust et al., 2010; Wang et al., 2014). The function of resin is to protect plants from invasion (Wolfe et al., 2009). Terpenoids are amongst the most diverse plant biomarkers, with more than 20,000 known compounds, and are associated with certain plant groups.

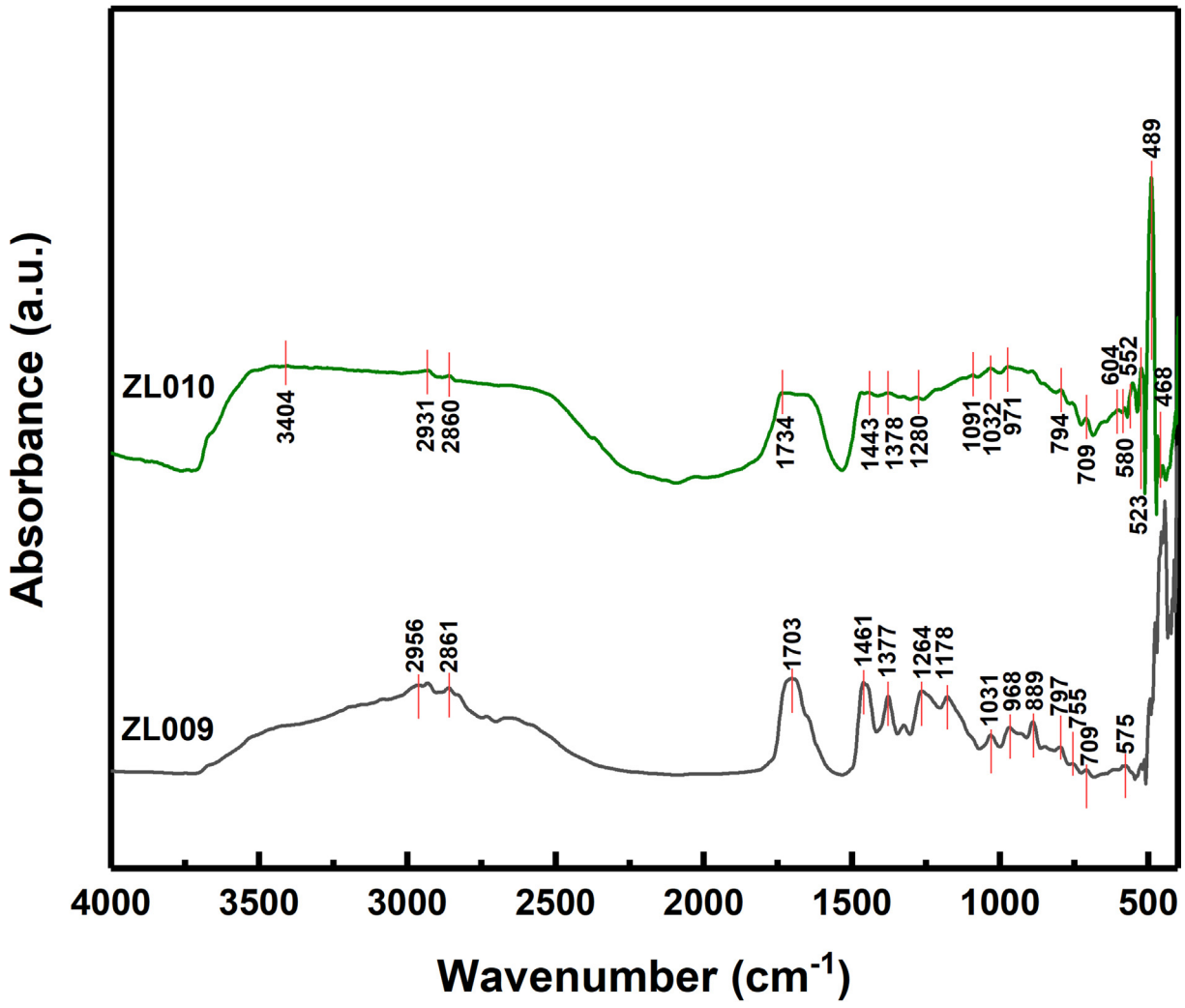

Fig. 6. The micro-FTIR features of Inner Mongolia amber.

Table 1
FTIR characteristics and comparisons of amber from different localities (based on Chen et al., 2019).

Band, cm^{-1}	Functional groups	Baltic amber	Burmese amber	Dominican amber	Fushun amber	Hailar amber
3082	C═C stretching	Weak	–	Weak	–	–
3060–3027	C═C stretching	–	–	–	–	–
2850–2926	H asymmetric stretching	Strong	Strong	Strong	Strong	Weak
1710–1737	C═O stretching	Strong	Strong	Strong	Strong	Medium
1696–1705	C═O stretching	–	Weak	Weak	Weak	Medium
1450–1458	H asymmetric bending	Strong	Strong	Strong	Strong	Medium
1373–1384	C–H symmetric bending	Strong	Strong	Strong	Strong	Medium
1220–1250	C–O stretching	–	–	Medium	–	Medium
1160–1220	C–O stretching	Medium	–	–	–	–
886–888	C═C deformations	Medium	–	Medium	Weak	Medium

Post burial chemical transformations notwithstanding, terpenoids in fossil resins and fossil plant remains still retain their characteristic chemical structures and can thus be used to interpret the taxonomic origins of the fossils and amber (Otto et al., 2002). For example, analyses of terpenoid compositions indicate the mid-Cretaceous Kachin amber derived from the conifer family Pinaceae, the Eocene Cambay amber of India and Zhangpu amber of China likely derived from the tropical angiosperm family Dipterocarpaceae, and the Eocene Baltic amber of Europe likely derived from the conifer family Sciadopityaceae (Santiago-Blay and Lambert, 2007; Dutta et al., 2009, 2011; Wang et al., 2021a). Other plant families that produce amber resins include Araucariaceae, Leguminosae, Burseraceae, Hamamelidaceae, Combretaceae, and the extinct conifer family Cheirolepidiaceae (Langenheim, 1969; Gough and Mills, 1972; Wolfe et al., 2016). Our study indicates that conifers of uncertain identity produced amber from the Hailar outcrops. Abundant gymnosperm fossils were discovered from the same strata, although the complex

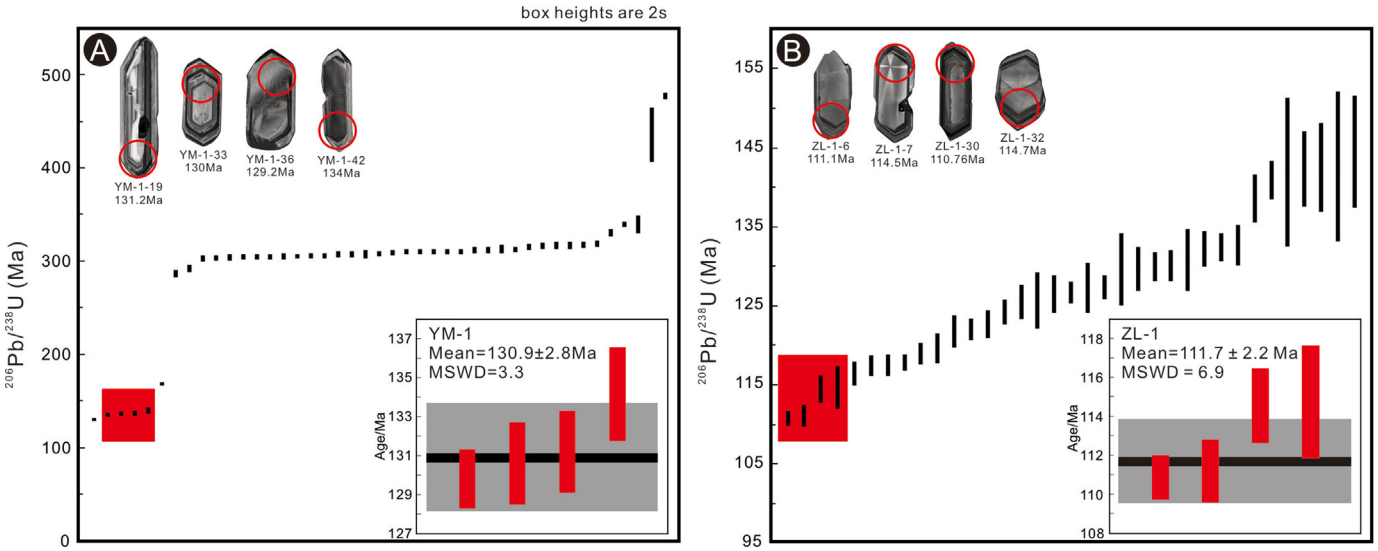

Fig. 7. Detrital zircon U–Pb geochronology of YM-1 from the Yimin Formation of the Zhalainuoer coal mine and ZL-1 from the Yimin Formation of the Yimin coal field. Cathodoluminescent (CL) images of representative zircons (red circle diameter = 40 μm) (A and C). MSWD—mean square of weighted deviates.

assemblages have yet to be identified (Wang et al., 2021b). Future constraints on plant assemblages from resin and fossils will further inform the reconstruction of ecosystems.

6.2. A window into the Cretaceous world

Amber-bearing deposits are among the most important *Konservat-Lagerstätten*, allowing to look into the details of past ecosystems (Antoine et al., 2006; Azar, 2007; Jarzembowski et al., 2008; Wang et al., 2014; Zheng et al., 2018). The variety of biological inclusions preserved in pristine, three-dimensional conditions within amber can contain different lines of evidence (e.g. Ross, 2014; Zheng et al., 2017, 2018). Studies demonstrate that delicate organisms are preserved in amber with life-like, microscopic fidelity (e.g. Ross, 2014; Wang et al., 2014; Chen et al., 2016; Xing et al., 2016a,b; Zheng et al., 2016, 2017, 2018; Grimaldi, 2019; Yu et al., 2019). Sometimes even complex behavior is preserved, such as camouflage, burrowing and related predation (Badano et al., 2018). As phylogenetic precision depends on the number of preserved taxa, fossils in amber have considerably resolved evolutionary parameters and relationships (e.g., Grimaldi and Agosti, 2000; Bauer et al., 2005; Perrichot et al., 2008; Pérez-de la Fuente and Peñalver, 2019; Zheng et al., 2019b; Zhao et al., 2021). For example, insects preserved with partially damaged dinosaur feathers from Kachin amber demonstrated that feather-feeding behaviors of insects originated in the mid-Cretaceous (Gao et al., 2019) although some researchers doubt this discovery (Grimaldi and Vea, 2021). The Early Cretaceous is among the most tectonically active sub-periods in Earth's history, with enhanced seafloor spreading, the breakup of Pangea, emplacement of a large igneous province, and other pervasive igneous activity (Larson and Erba, 1999; Ingle and Coffin, 2004; Wu et al., 2005). Many studies indicate an increase in oxygen levels during the Early Cretaceous (Wade et al., 2019) with some estimates exceeding present-day oxygen levels (Bergmann et al., 2004; Bond and Scott, 2010; Brown et al., 2012). Carbon dioxide levels during the Cretaceous are thought to have fluctuated and their relationship with temperature remains unclear (Huber et al., 2018). However, consensus holds that a global warm period occurred during the Early Cretaceous and peaked in the mid-Cretaceous (Huber et al., 2018; Tosolini et al., 2018). The average global temperature during the Cretaceous has been interpreted to be as much as 4.8 °C above present-day temperatures (Barron and Washington, 1982; Willis and McElwain, 2002). This was an important coal-forming period in the Earth's history (Ziegler et al., 1987; Price et al., 1995; Wendler and Wendler, 2016; Li et al., 2018 Song et al., 2017). Occurrences of coal seams are widely distributed around the world, and especially in northeast China. Coal petrography suggests a frequent recurrence of wildfire events during the deposition of the Yimin Formation and its underlying Damoguaihe Formation (Wang et al., 2021b).

The Hailar amber formed during a crucial period of coevolution between flowering plants and insects specifically entailed the radiation of angiosperms and the rapid diversification of insects accompanied by the massive extinction of older groups (Jarzembowski and Ross, 1993). The Cretaceous Terrestrial Revolution (KTR, Lloyd et al., 2008) represents the rapid expansion of flowering plants, herbivorous and social insects, dinosaurs, primitive birds, and early mammals by the Late Cretaceous (80 Ma).

The Early Cretaceous Jehol Biota is widely distributed throughout Central and Eastern Asia (Chen, 1988; Chen and Jin, 1999). Since the 1990s, the host Dabeigou, Huajiying, Yixian, and Jiufotang Formations (and correlative units) of the Liaoning Province, Hebei Province, and Inner Mongolia (all around northeast China) have yielded abundant terrestrial fossils (e.g., Wang et al., 2012; Zhang et al., 2015; Chang et al., 2014, 2017; Zheng et al., 2018; Wang et al., 2022). Fossils from these deposits are well preserved in lacustrine sediments with interbedded tuffs. Discoveries have significantly improved our understanding of the evolutionary history of several major groups (Chang et al., 2013; Zheng et al., 2021; Zhang et al., 2022; Zhou et al., 2022). Based on the age data presented here, the amber-bearing Yimin Formation equates to the classic Jehol deposit from the Yixian and Jiufotang formations in northeast China (Chang et al., 2009; Li et al., 2022; Yu et al., 2022).

Further investigations of the Hailar amber and the amber-bearing Yimin Formation can help constrain several fundamental questions. How did frequent wildfire events affect the local

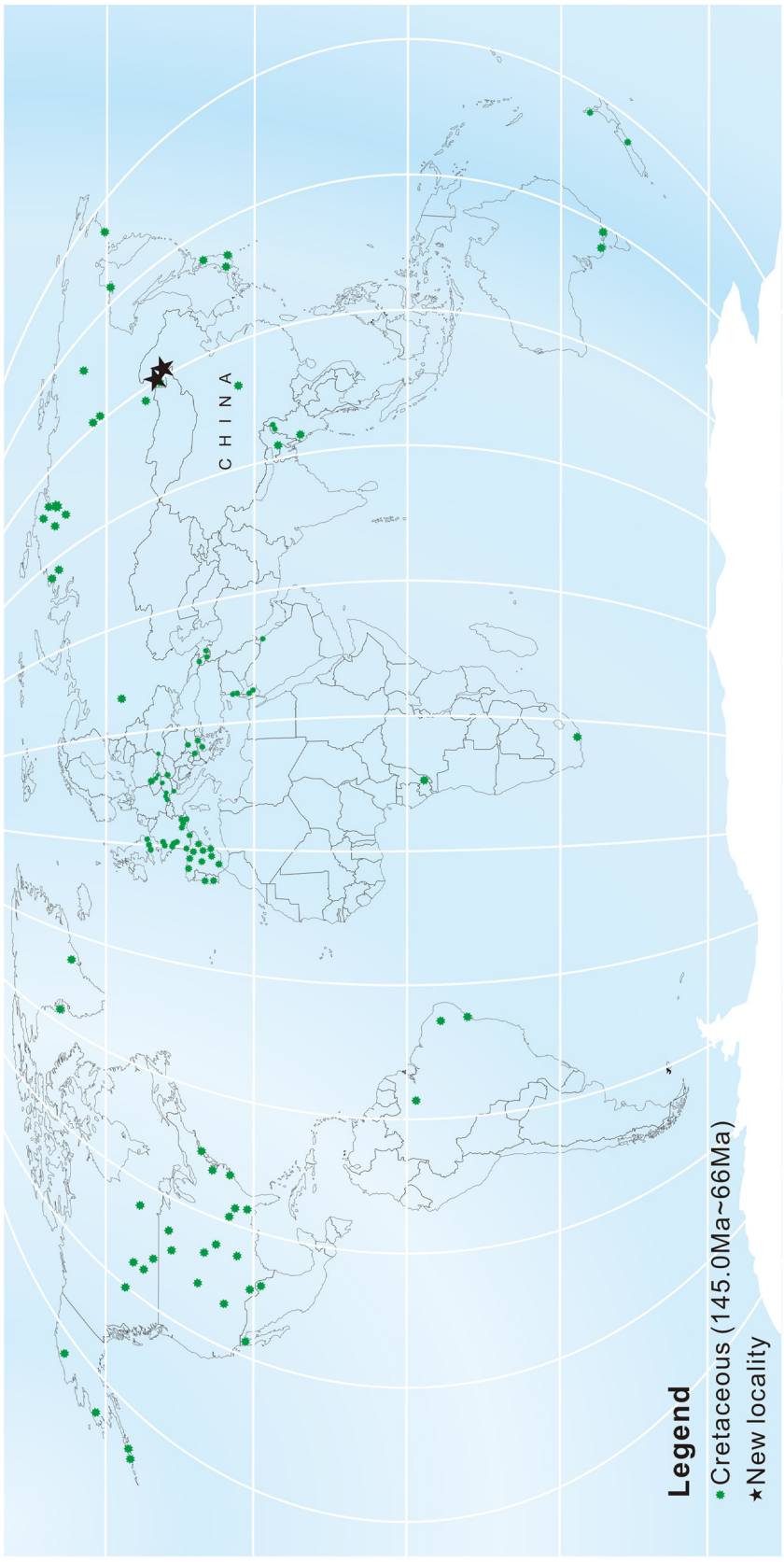

Fig. 8. The geographic locations of major Cretaceous fossil resins (modified from Rasnitsyn et al., 2016).

biodiversity? What were the biological recovery patterns after the recurrent wildfires? Did the amber preserve Jehol fossils within dated or datable depositional intervals, and did the geographic distribution of this amber approximately overlap with the second and third evolutionary stages of the Jehol Biota? If so, was the fossil assemblage different from those in the classic Jehol outcrops ~1000 km away?

6.3. Significant Cretaceous amber outcrops from other global localities

Abundant Cretaceous amber outcrops have been reported worldwide (Fig. 8). Our age results indicate that the *in situ* ambers from the Hailar Basin of northeast China were deposited in the Early Cretaceous, contemporary with Lebanese amber (Azar and Nel, 1998; Choufani et al., 2015) and Wealden amber (Nicholas et al., 1993). Formed in siliciclastic coastal and estuarine environments of northern Gondwana, the Lebanese amber contains a wide range of insect and plant inclusions indicating a dense forest growing in a warm tropical climate (Azar et al., 2011; Veltz et al., 2013). Three decades of intensive study of Lebanese amber inclusions have generated key records on biotic evolution and environments during the Mesozoic (Azar, 2007, 2012; Azar et al., 2011; Maksoud et al., 2017). For example, the discovery of multiple neonate green lacewing larva demonstrated that the hatching mechanism of modern green lacewings was established in the chrysopoid lineage by the Early Cretaceous (Pérez-de la Fuente et al., 2019). As another example, four well-preserved monotypic genera of Aleyrodidae elucidated whitefly diversity and morphological disparity in the Mesozoic (Drohojowska and Szwedo, 2015). The Wealden amber, derived from conifers, formed in forests not far to the north (~51°N) (Nicholas et al., 1993; Jarzembowski et al., 2008). This amber also contains abundant inclusions for reconstructing the Early Cretaceous ecosystems and Laurentian environments (Jarzembowski, 1995a,b; Sweetman and Insole, 2010). A previous study indicated that the Wealden paleoclimate may have resembled the Mediterranean, with hot dry summers alternating with wet winters (Allen et al., 1998). Wealden amber significantly provided an important record of insects that lived alongside the dinosaurs at the height of their diversity (Coram and Jarzembowski, 2021). The Hailar amber was deposited in the middle section of the eastern wing of the Mongolian arc-shaped fold belt formed between North China and the Siberian Plate. Early Cretaceous deposition in this basin records information on biodiversity and paleoclimate of this area.

7. Conclusions

Although China has a long history of amber usage and trade, systematic studies of amber are lacking. This study provides a brief literature review on Chinese amber deposits and their geological background. We also report FTIR composition and U−Pb age results for newly discovered amber from coal fields in Inner Mongolia of northern China. While inclusions do not apparently occur in the amber from the Hailar Basin described in this study, further investigations on amber and potential inclusions within the coal-bearing formations of the Hailar Basin will improve understanding of biological and environmental changes in Asia during the Early Cretaceous.

Acknowledgments

We sincerely thank Dr. Eduardo Koutsoukos and two anonymous reviewers for their constructive comments. We would like to thank Profs. Jacek Szwedo and Edmund Jarzembowski for their academic advice and help in the field, and Drs. He Wang, Qingqing Zhang and Hui Jiang, and Mr. Li Zhu for their help in the field. Thanks to Mr. Hongwang Li, Prof. Changquan Li, Dr. Zhenhui Luan, and the staff at the Yimin coalfield for their support. This research was supported by the Strategic Priority Research Program of the Chinese Academy of Sciences (XDB26000000), the HKU Seed Fund for Basic Research (202011159058) and the HK General Research Fund/RGC (17300718).

References

A, M., Zhang, F., Yang, S., Chen, H., Batt, G., Sun, M., Meng, Q., Zhu, D., Cao, R., Li, J., 2013. Early Cretaceous provenance change in the southern Hailar Basin, northeastern China and its implication for basin evolution. Cretaceous Research 40, 21−42.

Allen, P., Alvin, K.L., Andrews, J.E., Batten, D.J., Charlton, W.A., Cleevely, R.J., Ensom, P.C., Evans, S.E., Francis, J.E., Hailwood, E.A., Harding, I.C., 1998. Purbeck−Wealden (early Cretaceous) climates. Proceedings of the Geologists' Association 109, 197−236.

Alonso, J., Arillo, A., Barrón, E., Corral, J.C., Grimalt, J., López, J.F., López, R., Martínez-Delclòs, X., Ortuño, V., Peñalver, E., Trincão, P.R., 2000. A new fossil resin with biological inclusions in Lower Cretaceous deposits from Álava (Northern Spain, Basque-Cantabrian Basin). Journal of Paleontology 74, 158−178.

Antoine, P.O., De Franceschi, D., Flynn, J.J., Nel, A., Baby, P., Benammi, M., Calderón, Y., Espurt, N., Goswami, A., Salas-Gismondi, R., 2006. Amber from western Amazonia reveals Neotropical diversity during the middle Miocene. Proceedings of the National Academy of Sciences 103, 13595−13600.

Arillo, A., Subías, L.S., 2000. A new fossil oribatid mite, *Archaeorchestes minguezae* gen. nov., sp. nov. from the Spanish Lower Cretaceous amber. Description of a new family, Archaeorchestidae (Acariformes, Oribatida, Zetorchestoidea). Mitteilungen aus dem Geologisch-Paläontologischen Institut der Universität Hamburg 84, 231−236.

Arillo, A., Subías, L.S., 2002. Second fossil oribatid mite from the Spanish Lower Cretaceous amber. *Eupterotegaeus bitranslamellatus* n. sp. (Acariformes, Oribatida, Cepheidae). Acarologia 42, 403−406.

Azar, D., 2007. Preservation and accumulation of biological inclusions in Lebanese amber and their significance. Comptes Rendus Palevol 6, 151−156.

Azar, D., 2012. Lebanese amber: a "Guinness Book of Records". Annales Universitatis Paedagogicae Cracoviensis. Studia ad Didacticam Biologiae Pertinentia 2, 44−60.

Azar, D., Nel, A., 1998. Lebanese Lower Cretaceous amber. Meganeura 2, 18−20.

Azar, D., Dejax, J., Masure, E., 2011. Palynological analysis of amber-bearing clay from the Lower Cretaceous of Central Lebanon. Acta Geologica Sinica 85, 942−949.

Azar, D., Maksoud, S., Nammour, C., Nel, A., Wang, B., 2018. A new trogiid genus from lower Eocene Fushun amber (Insects: Psocodea: Trogiomorpha). Geobios 51, 101−106.

Azar, D., Maksoud, S., Cai, C., Huang, D., 2019. A new amber outcrop from the Lower Cretaceous of northeastern China. Palaeoentomology 2, 345−349.

Barron, E.J., Washington, W.M., 1982. Cretaceous climate: a comparison of atmospheric simulations with the geological record. Palaeogeography, Palaeoclimatology, Palaeoecology 40, 103−133.

Bauer, A.M., Böhme, W., Weitschat, W., 2005. An early Eocene gecko from Baltic amber and its implications for the evolution of gecko adhesion. Journal of Zoology 265, 327−332.

Badano, D., Engel, M.S., Basso, A., Wang, B., Cerretti, P., 2018. Diverse Cretaceous larvae reveal the evolutionary and behavioural history of antlions and lacewings. Nature Communications 9, 3257.

Bergmann, N., Lenton, T., Watson, A., 2004. A new model of biogeochemical cycling over Phanerozoic. American Journal of Science 304, 397−437.

Black, L.P., Kamo, S.L., Allen, C.M., Aleinikoff, J.N., Davis, D.W., Korsch, R.J., Foudoulis, C., 2003. TEMORA 1: a new zircon standard for Phanerozoic U−Pb geochronology. Chemical Geology 200, 155−170.

Bond, W.J., Scott, A.C., 2010. Fire and the spread of flowering plants in the Cretaceous. New Phytologist 188, 1137−1150.

Brazidec, M., Perrichot, V., 2022. The first fossil *Parascleroderma* (Hymenoptera: Bethylidae): a new species in mid-Miocene Zhangpu amber. Palaeoworld. https://doi.org/10.1016/j.palwor.2022.01.009.

Bray, P.S., Anderson, K.B., 2009. Identification of Carboniferous (320 million years old) Class Ic Amber. Science 326, 132−134.

Brown, S.A.E., Scott, A.C., Glasspool, I.J., Collinson, M.E., 2012. Cretaceous wildfires and their impact on the Earth System. Cretaceous Research 36, 162−190.

Cao, R., Zhu, D., Chen, J., Liu, H., Wang, Z., Wang, J., 2009. Structural evolution features of Hailar Basin-Tamtsag Basin. Petroleum Geology and Oilfield Development 28, 39−43.

Chang, S., Zhang, H., Hemming, S., Mesko, G., Fang, Y., 2013. $^{40}Ar/^{39}Ar$ age constraints on the Haifanggou and Lanqi formations: When did the first flowers bloom? Geological Society, London, Special Publications 378, 277−284.

Chang, S., Zhang, H., Renne, P.R., Fang, Y., 2009. High-precision $^{40}Ar/^{39}Ar$ age for the Jehol Biota. Palaeogeography, Palaeoclimatology, Palaeoecology 280, 94−104.

Chang, S., Hemming, S., Gao, K., Zhou, C., 2014. $^{40}Ar/^{39}Ar$ age constraints on Cretaceous fossil-bearing formations near the China-North Korea border. Palaeogeography, Palaeoclimatology, Palaeoecology 396, 93–98.
Chang, S., Gao, K., Zhou, C., Jourdan, F., 2017. New chronostratigraphic constraints on the Yixian Formation with implications for the Jehol Biota. Palaeogeography, Palaeoclimatology, Palaeoecology 487, 399–406.
Chen, P., 1988. Distribution and migration of the Jehol fauna with reference to the nonmarine Jurassic-Cretaceous boundary in China. Acta Palaeontologica Sinica 27, 659–683 (in Chinese with English summary).
Chen, P., Jin, F. (Eds.), 1999. The Jehol Biota. Palaeoworld 11, 1–342 (in Chinese with English summary).
Chen, J., Wang, D., Feng, J., Fu, G., Zhu, S., 2007. Late Cretaceous non-marine bivalves from the dinosaur egg-bearing strata in Xixia basin, Henan, China. Acta Palaeontologica Sinica 46, 299–313 (in Chinese with English summary).
Chen, J., Wang, B., Jarzembowski, E.A., 2016. Benefits of trade in amber fossils. Nature 532, 441.
Chen, D., Zeng, Q., Yuan, Y., Cui, B., Luo, W., 2019. Baltic amber or Burmese amber: FTIR studies on amber artifacts of Eastern Han Dynasty unearthed from Nanyang. Spectrochimica Acta Part A: Molecular and Biomolecular Spectroscopy 222, 117270.
Chen, Z., Li, C., Liu, X., 2022. New dustywings (Insecta: Neuroptera: Coniopterygidae) from the Miocene Zhangpu amber. Palaeoworld. https://doi.org/10.1016/j.palwor.2022.01.003.
Cheng, J., Shang, Y., 2015. Early Cretaceous palynological assemblage sequence and palaeoclimate research in Zhalainuoer Coalmine, Manzhouli, Inner Mongolia. Acta Geologica Sinica 54, 316–341 (in Chinese with English summary).
Choufani, J., El-Halabi, W., Azar, D., Nel, A., 2015. First fossil insect from Lower Cretaceous Lebanese amber in Syria (Diptera: Ceratopogonidae). Cretaceous Research 54, 106–116.
Coram, R.A., Jarzembowski, E.A., 2021. Immature insect assemblages from the Early Cretaceous (Purbeck/Wealden) of Southern England. Insects 12, 942.
Dong, W., Zhang, Y., Zhang, F., Cui, J., Chen, X., Zhang, S., Miao, L., Li, J., Shi, W., Li, Z., Huang, S., Li, H., 2015. Late Jurassic-Early Cretaceous continental convergence and intracontinental orogenesis in East Asia: a synthesis of the Yanshan Revolution. Journal of Asian Earth Sciences 114, 750–770.
Drohojowska, J., Szwedo, J., 2015. Early Cretaceous Aleyrodidae (Hemiptera: Sternorrhyncha) from the Lebanese amber. Cretaceous Research 52, 368–389.
Dutta, S., Mallick, M., Bertram, N., Greenwood, P.F., Matthews, R.P., 2009. Terpenoid composition and class of Tertiary resins from India. International Journal of Coal Geology 80, 44–50.
Dutta, S., Tripathi, S.M., Mallick, M., Matthews, R.P., Greenwood, P.F., Rao, M.R., Summons, R.E., 2011. Eocene out-of-India dispersal of Asian dipterocarps. Review of Palaeobotany and Palynology 166, 63–68.
Engel, M.S., Herhold, H., Davis, S., Wang, B., Thomas, J., 2021. Stingless bees in Miocene amber of southeastern China (Hymenoptera: Apidae). Journal of Melittology 105, 1–83.
Gao, T., Yin, X., Shih, C., Rasnitsyn, A.P., Xu, X., Chen, S., Wang, C., Ren, D., 2019. New insects feeding on dinosaur feathers in mid-Cretaceous amber. Nature Communications 10, 5424.
Gough, L.J., Mills, J.S., 1972. The composition of succinite (Baltic amber). Nature 239, 527–528.
Graham, S.A., Hendrix, M.S., Johnson, C.L., Badamgarav, D., Badarch, G., Amory, J., Porter, M., Barsbold, R., Webb, L.E., Hacker, B.R., 2001. Sedimentary record and tectonic implications of Mesozoic rifting in southeastern Mongolia. Geological Society of America Bulletin 113, 1560–1579.
Grimaldi, D., 2009. Pushing back amber production. Science 326, 51–52.
Grimaldi, D., 2019. Amber. Current Biology 29, 859–865.
Grimaldi, D., Agosti, D., 2000. A formicine in New Jersey Cretaceous amber (Hymenoptera: Formicidae) and early evolution of the ants. Proceedings of the National Academy of Sciences of the United States of America 97, 13678–13683.
Grimaldi, N., Vea, I.M., 2021. Insects with 100 million-year-old dinosaur feathers are not ectoparasites. Nature Communications 12, 1469.
Guo, B., Shao, L., Zhang, Q., 2014. Sequence stratigraphy and coal accumulation of the lower Cretaceous coal measures in Hailar Basin. Journal of Palaeogeography 16, 631–640.
Guo, B., Shao, L., Hilton, J., Wang, S., Zhang, L., 2018. Sequence stratigraphic interpretation of peatland evolution in thick coal seams: examples from Yimin Formation (Early Cretaceous), Hailar Basin, China. International Journal of Coal Geology 196, 211–231.
Hong, Y., 2002. Amber Insects of China. Beijing Scientific and Technological Publishing House, Beijing (in Chinese).
Hong, Y., Yang, T., Wang, S., Wang, S., Li, Y., Sun, M., Sun, H., Tu, N., 1974. Stratigraphy and Palaeontology of Fushun coal-field, Liaoning Province. Acta Geologica Sinica 2, 113–149.
Hou, Y., Zhu, D., Ren, Y., Zhuang, X., 2008. Tectonic evolution and its control on sedimentation and hydrocarbon accumulation in Beier Depression. Geotectonica et Metallogenia 32, 300–307.
Huang, Q., Zhao, L., Lu, Z., Dang, Y., Wang, L., Kong, H., 2006. Sporopollen fossil of the Damoguaile Formation and its age in Hailar Basin, Inner Mongolia. Geological Science and Technology Information 25, 19–26.
Huber, B.T., MacLeid, K.G., Watkins, D.K., Coffin, M.F., 2018. The rise and fall of the Cretaceous Hot Greenhouse climate. Global and Planetary Change 167, 1–23.
Huo, W., Zhao, D., 2007. Foreign Cultural Exchanges in Southwest China during the Warring States Period, Qin and Han Dynasties. Bashu Publishing House, Chengdu, China (in Chinese).
Ingle, S., Coffin, M.F., 2004. Impact origin for the greater Ontong Java Plateau? Earth and Planetary Science Letters 218, 123–134.
Inner Mongolia Autonomous Regional Bureau of Geology and Mineral Resources, 1996. Lithologic Stratigraphy of Inner Mongolia Autonomous Region. China University of Geosciencs Press, Beijing, p. 344 (in Chinese).
Jaffey, A.H., Flynn, K.F., Glendenin, L.E., Bentley, W.T., Essling, A.M., 1971. Precision measurement of half-lives and specific activities of U 235 and U 238. Physical Review C 4, 1889.
Jarzembowski, E.A., 1995a. The first insects in Cretaceous (Wealden) amber from the UK. Geology Today 11, 41–42.
Jarzembowski, E.A., 1995b. Early Cretaceous insect fauna and palaeoenvironment. Cretaceous Research 16, 681–693.
Jarzembowski, E.A., Ross, A., 1993. Time flies: the geological record of insects. Geology Today 9, 218–223.
Jarzembowski, E.A., Azar, D., Nel, A., 2008. A new chironomid (Insecta: Diptera) from Wealden amber (Lower Cretaceous) of the Isle of Wight (UK). Geológica Acta 6, 285–291.
Ji, Z., Meng, Q., Wan, C., Zhu, D., Ge, W., Zhang, Y., Yang, H., Dong, Y., Jing, Y., 2019. Generation of late Mesozoic felsic volcanic rocks in the Hailar Basin, northeastern China in response to overprinting of multiple tectonic regimes. Scientific Reports 9, 1–15.
Ji, Z., Wan, C., Meng, Q., Zhu, D., Ge, W., Zhang, L., Yang, H., Dong, Y., Jing, Y., 2020. Geochronostratigraphic framework of late Mesozoic terrestrial strata in the Hailar-Tamtsag Basin, Northeast China and its geodynamic implication. Geological Journal 55, 5197–5215.
Ji, Z., Zhang, Y., Wan, C., Ge, W., Yang, H., Dong, Y., Jing, Y., 2021. Recycling of crustal materials and implications for lithospheric thinning: Evidence from Mesozoic volcanic rocks in the Hailar-Tamstag Basin, NE China. Geoscience Frontiers 12, 101184.
Jia, R., Liu, B., Fu, X., Gong, L., Liu, Z., 2019. Transformation mechanism of a fault and its associated microstructures in low-porosity rocks: a case study in the Tanan Depression in the Hailar-Tamstag Basin. Journal of Marine Science and Engineering 7, 286.
Langenheim, J.H., 1969. Amber: a botanical inquiry. Science 163, 1157–1169.
Larson, R.L., Erba, E., 1999. Onset of the mid-Cretaceous greenhouse in the Barremian-Aptian igneous events and the biological, sedimentary, and geochemical responses. Paleoceanography 14, 663–678.
Laufer, B., 1906. Historical jottings on Amber in Asia. Memoirs of the American Anthropological Association 1, 215–244.
Li, Z., Wang, D., Lv, D., Li, Y., Liu, H., Wang, P., Liu, Y., Liu, J., Li, D., 2018. The geologic settings of Chinese coal deposits. International Geology Review 60, 548–578.
Li, X., Mancgester, S.R., Xiao, L., Wang, Q., Hu, Y., Sun, B., 2021. Ormosia (Fabaceae: Faboideae) from the Miocene of southeastern China support historical expansion of the tropical genus in East Asia. Historical Biology 33, 3561–3578.
Li, Y., Jicha, B.R., Yu, Z., Wu, H., Wang, X., Singer, B., He, H., Zhou, Z., 2022. Rapid preservation of Jehol Biota in Northeast China from high precision $^{40}Ar/^{39}Ar$ geochronology. Earth and Planetary Science Letters 594, 117718.
Liu, Q., Zeng, G., Lian, X., Fu, Y., Cai, C., Huang, D., 2021. A new amber outcrop from Oligocene Nanning Basin of Guangxi, southern China. Palaeontomology 4, 326–330.
Lloyd, G.T., Davis, K.E., Pisani, D., Tarver, J.E., Ruta, M., Sakamoto, M., Hone, D.W.E., Jennings, R., Benton, M., 2008. Dinosaurs and the Cretaceous Terrestrial Revolution. Proceedings of the Royal Society B 275, 2483–2490.
Maksoud, S., Azar, D., Granier, B., Gèze, 2017. New data on the age of the Lower Cretaceous amber outcrops of Lebanon. Palaeoworld 26, 331–338.
Meng, Q., Hu, J., Jin, J., Zhang, Y., Xu, D., 2003. Tectonics of the late Mesozoic wide extensional basin system in the China-Mongolia border region. Basin Research 15, 397–415.
Nicholas, C.J., Henwood, A.A., Simpson, M., 1993. A new discovery of early Cretaceous (Wealden) amber from the Isle of Wight. Geological Magazine 30, 847–850.
Otto, A., White, J.D., Simoneit, B.R., 2002. Natural product terpenoids in Eocene and Miocene conifer fossils. Science 297, 1543–1545.
Ouyang, H., Mao, J., Zhou, Z., Su, H., 2015. Late Mesozoic metallogeny and intracontinental magmatism, southern Great Xing'an Range, northeastern China. Gondwana Research 27, 1153–1172.
Pérez-de la Fuente, R., Peñalver, E., 2019. A mantidfly in Cretaceous Spanish amber provides insights into the evolution of integumentary specialisations on the raptorial foreleg. Scientific Reports 9, 13248.
Pérez-de la Fuente, R., Engel, M.S., Azar, D., Peñalver, E., 2019. The hatching mechanism of 130-million-year-old insects: an association of neonates, egg shells and egg bursters in Lebanese amber. Palaeontology 62, 547–559.
Perrichot, V., Marion, L., Neraudeau, D., Vullo, R., Tafforeau, P., 2008. The early evolution of feathers: fossil evidence from Cretaceous amber in France. Proceedings of the Royal Society B 275, 1197–1202.
Ping, C., 1931. On a Blattoid insect in the Fushun amber. Bulletin of the Geological Society of China 11, 205–207.
Price, G.B., Sellwood, B.W., Valdes, P.J., 1995. Sedimentological evaluation of general circulation model simulations for the "greenhouse" Earth: Cretaceous and Jurassic case studies. Sedimentary Geology 100, 159–180.
Pu, H., Zelentisky, D.K., Lu, J., Currie, P.J., Carpenter, K., Xu, L., Koppelhus, E.B., Jia, S., Xiao, L., Chuang, H., Li, T., Kundrat, M., Shen, C., 2017. Perinate and eggs of a giant caenagnathid dinosaur from the Late Cretaceous of central China. Nature Communications 8, 14952.

Pu, R., Wu, H., 1985. The palynological assemblages of the Xinganling and Zhalainuoer in Xinganling region, northeastern China and their stratigraphical significance. Bulletin of the Shenyang Institute of Geology and Mineral Resources, Chinese Academy of Geological Sciences 11, 47–113 (in Chinese with English summary).
Qin, C., Sun, A., 2016. A tentative identification and sources investigation of China's ancient amber beads. Acta Petrologica et Mineralogica 35, 127–136 (in Chinese with English abstract).
Rasnitsyn, A.P., Bashkuev, A.S., Kopylov, D.S., Lukashevich, E.D., Ponomarenko, A.G., Popov, Y.A., Rasnitsyn, D.A., Ryzhkova, O.V., Sidorchuk, E.A., Sukatsheva, I.D., Vorontsov, D.D., 2016. Sequence and scale of changes in the terrestrial biota during the Cretaceous (based on materials from fossil resins). Cretaceous Research 61, 234–255.
Ross, A., 2014. Palaeontology: Chinese amber insects bridge the gap. Current Biology 24, 623–624.
Rust, J., Singh, H., Rana, R.S., McCann, T., Singh, L., Anderson, K., Sarkar, N., Nascimbene, P.C., Stebner, F., Thomas, J.C., Kraemer, M.S., 2010. Biogeographic and evolutionary implications of a diverse paleobiota in amber from the early Eocene of India. Proceedings of the National Academy of Sciences 107, 18360–18365.
Santiago-Blay, J.A., Lambert, J.B., 2007. Amber's Botanical Origins Revealed: Large collections of the substances exuded by trees today may help to track backward from amber samples to the ancient plants that produced them. American Scientist 95, 150–157.
Schmidt, A.R., Ragazzi, E., Coppellotti, O., Roghi, G., 2006. A microworld in Triassic amber. Nature 444, 835.
Shi, G., Dutta, S., Paul, S., Wang, B., Jacques, F.M.B., 2014a. Terpenoid compositions and botanical origins of late Cretaceous and Miocene amber from China. PLoS One 9, e111303.
Shi, G., Jacques, F.M., Li, H., 2014b. Winged fruits of Shorea (Dipterocarpaceae) from the Miocene of Southeast China: evidence for the northward extension of dipterocaps during the Mid-Miocene Climate Optimum. Review of Palaeobotany and Palynology 200, 97–107.
Sláma, J., Košler, J., Condon, D.J., Crowley, J.L., Gerdes, A., Hanchar, J.M., Horstwood, M.S., Morris, G.A., Nasdala, L., Norberg, N., Schaltegger, U., 2008. Plešovice zircon—a new natural reference material for U–Pb and Hf isotopic microanalysis. Chemical Geology 249, 1–35.
Song, Y., Liu, Z., Bechtel, A., Sachsenhofer, R.F., Groß, D., Meng, Q., 2017. Paleoenvironmental reconstruction of the coal- and oil shale-bearing interval in the lower Cretaceous Muling Formation, Laoheishan Basin, Northeast China. International Journal of Coal Geology 172, 1–18.
Song, J., Liu, Z., Wang, C., Gao, X., Liu, X., 2019. Multistage structural deformation of a superimposed basin system and its tectonic response to regional geological evolution: a case study from the Late Jurassic-Early Cretaceous Tanan depression, Hailar-Tamtsag basin. Marine and Petroleum Geology 110, 1–20.
Stebner, F., Szadziewski, R., Singh, H., Gunkel, S., Rust, J., 2017. Biting midges (Diptera: Ceratopogonidae) from Cambay amber indicate that the Eocene fauna of the Indian subcontinent was not isolated. PLoS One 12, e169144.
Steiger, R.H., Jäger, E., 1977. Subcommission on geochronology: convention on the use of decay constants in geo-and cosmochronology. Earth and Planetary Science Letters 36, 359–362.
Sun, M., Chen, H., Milan, L.A., Wilde, S.A., Jourdan, F., Xu, Y., 2018. Continental Arc and Back-migration in eastern NE China: new constraints on Cretaceous Paleo-Pacific Subduction and Rollback. Tectonics 37, 3893–3915.
Suo, Y., Li, S., Cao, X., Wang, X., Somerville, I., Wang, G., Wang, P., Liu, B., 2020. Mesozoic-Cenozoic basin inversion and geodynamics in East China: a review. Earth-Science Reviews 210, 103357.
Sweetman, S., Insole, A.,M., 2010. The plant debris beds of the Early Cretaceous (Barremian) Wessex Formation of the Isle of Wight, southern England: their genesis and palaeontological significance. Palaeogeography, Palaeoclimatology, Palaeoecology 292, 409–424.
Tian, Y., Shaw, D., Schneider, S., 2018. Oligocene fossil assemblages from Lake Nanning (Yongning Formation; Nanning Basin, Guangxi Province, SE China): biodiversity and evolutionary implications. Palaeogeography, Palaeoclimatology, Palaeoecology 505, 100–119.
Tosolini, A.M.P., Korasides, V.A., Wagstaff, B.E., Cantrill, D.J., Gallagher, S.J., Norvick, M.S., 2018. Palaeoenvironments and palaeoecommunities from Lower Cretaceous high-latitude sites, Otway Basin, southeastern Australia. Palaeogeography, Palaeoclimatology, Palaeoecology 496, 62–84.
Veltz, I., Paicheler, J., Maksound, S., Gèze, R., Azar, D., 2013. Context and genesis of the Lebanese amberiferous paleoenvironments at the Jurassic-Cretaceous transition. Terrestrial Arthropod Reviews 6, 11–26.
Wade, D.C., Abraham, N.L., Fransworth, A., Valdes, P.J., Bragg, F., Archibald, A.T., 2019. Simulating the climate response to atmospheric oxygen variability in the Phanerozoic: a focus on the Holocene, Cretaceous and Permian. Climate of the Past 15, 1463–1483.
Wan, C., 2006. Cretaceous Palynological Flora in Hailar Basin. Jilin University, Changchun, China (in Chinese with English abstract).
Wan, C., Qiao, X., Xu, Y., Sun, Y., Ren, Y., Jin, Y., Gao, P., Liu, T., 2005. Sporopollen assemblages from the Cretaceous Yimin Formation of the Hailar Basin, Inner Mongolia, China. Acta Geologica Sinica 79, 459–470.
Wang, D., Chen, P., Chen, J., Cao, M., Pan, H., 2006. Discovery of invertebrate fossils from the dinosaurian egg-bearing strata in the Xixia basin of Henan, China. Acta Palaeontologica Sinica 45, 494–497 (in Chinese with English summary).
Wang, L., Sun, Y., Qiao, X., Xue, Y., Jin, Y., 2008. The Early Cretaceous palynologic palaeoclimate of Hailar Basin. Petroleum Geology & Oilfield Development in Daqing 27, 38–42.
Wang, B., Zhang, H., Azar, D., 2011. The First Psychodidae (Insecta: Diptera) from the Lower Eocene Fushun Amber of China. Journal of Paleontology 85, 1154–1159.
Wang, Y., Sha, J., Pan, Y., Zhang, X., Rao, X., 2012. Non-marine Cretaceous ostracod assemblages in China: a preliminary review. Journal of Stratigraphy 36, 289–299.
Wang, B., Rust, J., Engel, M.S., Szwedo, J., Dutta, S., Nel, A., Fan, Y., Meng, F., Shi, G., Jarzembowski, E.A., Wappler, T., Stebner, F., Fang, Y., Mao, L., Zhang, D., Zhang, H., 2014. A diverse paleobiota in Early Eocene Fushun amber from China. Current Biology 24, 1606–1610.
Wang, H., Dutta, S., Kelly, R.S., Rudra, A., Li, S., Zhang, Q., Zhang, Q., Wu, Y., Cao, M., Wang, B., Li, J., Zhang, H., 2018. Amber fossil reveal the Early Cenozoic dipterocarp rainforest in central Tibet. Palaeoworld 27, 506–513.
Wang, B., Shi, G., Xu, C., Spicer, R.A., Perrichot, V., Schmidt, A.R., Feldberg, K., Heinrichs, J., Cheny, C., Pang, H., Liu, X., Gao, T., Wang, X., Slipinski, A., Solorzano-Kraemer, M.M., Heads, S.W., Thomas, M.J., Sadowski, E., Szwedo, J., Azar, D., Nel, A., Liu, Y., Chen, J., Zhang, Q., Zhang, Q., Luo, C., Yu, T., Zheng, D., Zhang, H., Engel, M.S., 2021a. The mid-Miocene Zhangpu biota reveals an outstanding rich rainforest biome in East Asia. Science Advances 7, eabg0625.
Wang, S., Shao, L., Li, J., Li, J., Jones, T., Zhu, M., Zhou, J., 2021b. Coal petrology of the Yimin Formation (Albian) in the Hailar Basin, NE China: Paleoenvironments and wildfires during peat formation. Cretaceous Research 124, 104815.
Wang, Z., Shi, G., Sun, B., Jia, H., Dong, C., Yin, S., Wu, X., 2021c. A new Cercis (Leguminosae) from the middle Miocene of Fujian, China. Historical Biology 34, 94–101.
Wang, J., Zhou, C., Jourdan, F., Chang, S., 2022. Jehol Biota from the Jiaolai Basin of Shandong, North China: review and new perspectives. Geological Society, London, Special Publications 521, 225–236.
Wendler, J.E., Wendler, I., 2016. What drove sea-level fluctuations during the mid-Cretaceous greenhouse climate. Palaeogeography, Palaeoclimatology, Palaeoecology 441, 412–419.
Wiedenbeck, M., Alle, P., Corfu, F., Griffin, W.L., Meier, M., Oberli, F.V., von Quadt, A., Roddick, J.C., Spiegel, W., 1995. Three natural zircon standards for U-Th-Pb, Lu-Hf, trace element and REE analyses. Geostandards Newsletter 19, 1–23.
Willis, K.J., McElwain, J.C., 2002. The Evolution of Plants. Oxford University Press, Oxford, p. 378.
Wolfe, A.P., Tappert, R., Muehlenbachs, K., Boudreau, M., McKellar, R.C., 2009. A new proposal concerning the botanical origin of Baltic amber. Proceedings of the Royal Society B: Biological Sciences 276, 3403–3412.
Wolfe, A.P., McKellar, R.C., Tappert, R., Sodhi, R.N.S., Muehlenbachs, K., 2016. Bitterfeld amber is not Baltic amber: three geochemical tests and further constraints on the botanical affinities of succinite. Review of Palaeobotany and Palynology 225, 21–32.
Wu, F., Lin, J., Wilde, S.A., Zhang, X., Yang, J., 2005. Nature and significance of the Early Cretaceous giant igneous event in eastern China. Earth and Planetary Science Letters 233, 103–119.
Wu, H., Huang, Q., Dang, Y., Kong, H., Wang, L., 2006. Achievements in the study on Cretaceous biostratigraphy of the Hailar Basin, Inner Mongolia. Acta Palaeontologica Sinica 45, 283–291 (in Chinese with English abstract).
Wu, G., Duan, A., Liu, Y., Mao, J., Ren, R., Bao, Q., He, B., Liu, B., Hu, W., 2015. Tibetan Plateau climate dynamics: recent research progress and outlook. National Science Review 2, 100–116.
Xia, Y., Lu, S., Haung, F., 2017. Iron and Zinc isotope fractionation during magmatism in the continental crust: evidence from bimodal volcanic rocks from Hailar basin, NE China. Geochimica et Cosmochimica Acta 213, 35–46.
Xing, L., McKellar, R.C., Xu, X., Li, G., Bai, M., Persons, W.S., Miyashita, T., Benton, M., Zhang, J., Wolfe, A.P., Yi, Q., Tseng, K., Ran, H., Currie, P.J., 2016a. A feathered dinosaur tail with primitive plumage trapped in mid-Cretaceous amber. Current Biology 26, 3352–3360.
Xing, L., McKellar, R.C., Wang, M., Bai, M., O'Connor, J.K., Benton, M.J., Zhang, J., Wang, Y., Tseng, K., Lockley, M.G., Li, G., Zhang, W., Xu, X., 2016b. Mummified precocial bird wings in mid-Cretaceous Burmese amber. Nature Communications 7, 12089.
Xu, L., Xie, J., Zhang, S., Choi, S., Kim, N., Gao, D., Jin, X., Jia, S., Gao, Y., 2022. Fossil turtle eggs from the Upper Cretaceous Gaogou Formation, Xiaguan-Gaoqiu Basin, Neixiang County, Henan Province, China: interpretation of the transformation from aragonite to calcite in fossil turtle eggshell. Cretaceous Research 134, 105166.
Yu, T., Kelly, R., Mu, L., Ross, A., Kennedy, J., Broly, P., Xia, F., Zhang, H., Wang, B., Dilcher, D., 2019. An ammonite trapped in Burmese amber. Proceedings of the National Academy of Sciences 116, 11345–11350.
Yu, Z., Dong, L., Huyskens, M.H., Yin, Q., Wang, Y., Deng, C., He, H., 2022. The exceptionally preserved Early Cretaceous "Moqi Fauna" from eastern Inner Mongolia, China, and its age relationship with the Jehol Biota. Palaeogeography, Palaeoclimatology, Palaeoecology 589, 110824.
Zhang, C., Long, Y., 1995. Features of Sedimentary Facies and Oil/Gas Distribution in Hailar Basin. Petroleum Industry Press, Beijing, pp. 1–8 (in Chinese).
Zhang, X., Guo, Y., Zeng, Z., Fu, Q., Pu, J., 2015. Dynamic evolution of the Mesozoic-Cenozoic basins in the northeastern China. Earth Science Frontiers 22, 88–98 (in Chinese with English abstract).
Zhang, Q., Nel, A., Azar, D., Wang, B., 2016. New Chinese psocids from Eocene Fushun amber (Insecta: Psocodea). Alcheringa: An Australian Journal of Palaeontology 40, 366–372.

Zhang, L., Zheng, D., Chang, S., Fang, Y., Li, Y., Wang, B., Zhang, H., 2022. New age constraints on the early Jehol Biota of Luanping, northeastern China. Palaeogeography, Palaeoclimatology, Palaeoecology 585, 110748.
Zhao, Z., Shih, C., Gao, T., Ren, D., 2021. Termite communities and their early evolution and ecology trapped in Cretaceous amber. Cretaceous Research 117, 104612.
Zheng, W., Jin, X., Xu, X., 2015. A psittacosaurid-like neoceratopsian from the Upper Cretaceous of central China and its implications for basal ceratopsian evolution. Scientific Reports 5, 14190.
Zheng, D., Zhang, Q., Chang, S., Wang, B., 2016. A new damselfly (Odonata: Zygoptera: Platystictidae) from mid-Cretaceous Burmese amber. Cretaceous Research 63, 142–147.
Zheng, D., Nel, A., Jarzembowski, E.A., Chang, S., Zhang, H., Xia, F., Liu, H., Wang, B., 2017. Extreme adaptations for probable visual courtship behaviour in a Cretaceous dancing damselfly. Scientific Reports 7, 44932.
Zheng, D., Chang, S., Perrichot, V., Dutta, S., Rudra, A., Mu, L., Kelly, R.S., Li, S., Zhang, Q., Wong, J., Wang, J., Wang, H., Fang, Y., Zhang, H., Wang, B., 2018. A Late Cretaceous amber biota from central Myanmar. Nature Communications 9, 1–6.
Zheng, D., Shi, G., Hemming, S., Zhang, H., Wang, W., Wang, B., Chang, S., 2019a. Age constraints on a Neogene tropical rainforest in China and its relation to the Middle Miocene Climatic Optimum. Palaoegeography, Palaeoclimatology, Palaeoecology 518, 82–88.
Zheng, D., Nel, A., Jarzembowski, E.A., Chang, S., Zhang, H., Wang, B., 2019b. Exceptionally well-preserved dragonflies (Insecta: Odonata) in Mexican amber. Alcheringa: An Australian Journal of Palaeontology 43, 157–164.
Zheng, D., Wang, H., Li, S., Wang, B., Jarzembowski, E.A., Dong, C., Fang, Y., Teng, X., Yu, T., Yang, L., Li, Y., Zhao, X., Xue, N., Chang, S., Zhang, H., 2021. Synthesis of a chrono-and biostratigraphic framework for the Lower Cretaceous of Jiuquan, NW China: implications for major evolutionary events. Earth-Science Reviews 213, 103474.
Zhou, S.Q., Zhao, S.L., 2005. Initial study on the Xixia-Neixiang amber deposit of Henan. Mineral Resources and Geology 19, 57–59.
Zhou, Y., Ji, Y., Pigott, J.D., Meng, Q., Wan, L., 2014. Tectono-stratigraphy of Lower Cretaceous Tanan sub-basin, Tamtsag Bain, Mongolia: sequence architecture, depositional systems and controls on sediment infill. Marine and Petroleum Geology 49, 176–202.
Zhou, C.F., Yu, D., Zhu, Z., Andres, B., 2022. A new wing skeleton of the Jehol tapejarid Sinopterus and its implications for ontogeny and paleoecology of the Tapejaridae. Scientific Reports 12, 10159.
Zhu, J., Meng, Q., Feng, Y., Yuan, H., Wu, F., Wu, H., Wu, G., Zhu, R., 2019. Decoding stratigraphic evolution of the Hailar Basin: implications for the late Mesozoic tectonics of NE China. Geological Journal 55, 1–13.
Ziegler, A.M., Raymond, A.L., Gierlowski, T.C., Horrell, M.A., Rowley, D.B., Lottes, A.L., 1987. Coal, climate and terrestrial productivity: the present and early Cretaceous compared. Geological Society, London, Special Publications 32, 25–49.

Appendix A. Supplementary data

Supplementary data to this article can be found online at https://doi.org/10.1016/j.cretres.2022.105472.